OMIP

OMIP 083: A 21-marker 18-color flow cytometry panel for in-depth phenotyping of human peripheral monocytes

Kathryn E. Hally[1,2,3] ⓘ | **Laura Ferrer-Font**[4] ⓘ | **Katherine R. Pilkington**[5] ⓘ | **Peter D. Larsen**[1,2,3] ⓘ

[1]Department of Surgery and Anaesthesia, The University of Otago, Wellington

[2]School of Biological Sciences, Victoria University of Wellington, Wellington

[3]Wellington Cardiovascular Research Group, Wellington

[4]Hugh Green Cytometry Centre, Malaghan Institute of Medical Research, Wellington, New Zealand

[5]Cytek Biosciences, Inc, Fremont, California, United States

Correspondence
Kathryn Hally, Department of Surgery and Anaesthesia, University of Otago, 23A Mein Street, Newtown, Wellington, New Zealand.
Email: kathryn.hally@otago.ac.nz

PURPOSE AND APPROPRIATE SAMPLE TYPES

This 21-marker, 18-color panel was developed to accurately delineate monocyte subsets by manual gating and, once successfully gated, to characterize monocyte function in-depth. This panel was optimized on human peripheral blood mononuclear cells (PBMCs) density-separated from whole blood drawn into Cyto-Chex blood collection tubes (BCTs; Streck, La Vista, NE) from healthy adults. All samples were analyzed on a three-laser (violet-blue-red) Aurora full spectrum flow cytometer (Cytek Biosciences, Fremont, CA). Deep phenotyping was achieved by minimizing the number of channels used to exclude nonmonocyte cells and maximizing the number of markers included to monitor monocyte immune status. This panel was specifically designed to interrogate cell-surface expression of monocyte-centric antigens to reduce handling time and complexity, which are desirable characteristics of a clinically applicable protocol. Although not tested on cryopreserved PBMCs or with alternative BCTs, we anticipate that this panel could be used on these sample types with minimal optimization. For optimal staining, we recommend the use of density-separated PBMCs over red blood cell (RBC)-lysed whole blood. In supplementary material, we highlight our step-wise troubleshooting to achieve optimal staining of this panel.

1 | BACKGROUND

Acute and chronic inflammatory diseases are often associated with significant risk of progression and recurrence. This risk is amplified by the lack of accurate clinical risk-stratification tools for prediction of survival from morbidity and mortality. Due to their heterogeneity and plasticity, the role of monocytes in propagating and maintaining many inflammatory diseases is well-established. Interrogating the dynamics of monocyte phenotype in these clinical contexts may provide a tool both for better understanding of pathology and for predicting disease course. To this end, we have developed a 21-marker, 18-color immunophenotyping panel for deep monocyte analysis in human peripheral blood (Table 1). This is the second optimized multicolor immunofluorescence panel (OMIP) to utilize full spectrum flow cytometry [1]. Analysis of the full spectrum of each fluorochrome as well as analysis of the autofluorescence spectrum of cells-of-interest allows for the use of fluorochrome combinations that are unable to be differentiated by conventional cytometry and increases the resolution of cell populations [2]. Of particular interest to the aims of this OMIP, which contains many markers co-expressed on monocytes, the reduced level of spreading error seen with full spectrum flow cytometry aided in resolving issues of spread with co-expressed markers.

Many published OMIPs aim to enumerate many cellular subtypes from blood [1, 3–7] (Table 1). However, there is also a need to focus

on deep phenotyping of individual subsets that are implicated in disease progression and survival. While these deep phenotyping panels exist for other peripheral subsets (namely T cells, B cells and dendritic cells [DCs]), there remains room to introduce such a flow cytometry-based panel for peripheral innate subsets, such as monocytes and neutrophils. Here, we expand on existing OMIPs by presenting a monocyte-centric panel that is designed to exclude nonmonocyte cells, identify and delineate four monocyte subsets and, once identified, to phenotypically characterize each subset.

Circulating human monocytes are conventionally divided into three subsets as follows [8, 9]: classical ($CD14^{++}/CD16^-$), intermediate ($CD14^+/CD16^+$), and nonclassical ($CD14^-/CD16^{++}$). These subsets differ in their function: classical monocytes contribute to the host's pro-inflammatory defense mechanisms, while intermediate monocytes are attuned toward antigen presentation, and nonclassical monocytes play a role in vascular patrolling and surveillance [18, 19].

Here, we expand on these definitions by further subsetting non-classical monocytes based on expression of SLAN (6-sulfo LacNAc), a carbohydrate modification of P-selectin glycoprotein ligand-1 (PSGL-1). Within nonclassical monocytes, we can define a $SLAN^+$ ($CD14^-/CD16^{++}/SLAN^+$) and a $SLAN^-$ ($CD14^-/CD16^{++}/SLAN^-$) subset [10–13]. $SLAN^+$ nonclassical monocytes been shown to be both phenotypically and functionally different from their $SLAN^-$ counterparts [11, 13]. Originally classified as DCs, $SLAN^+$ nonclassical monocytes are now recognized as a bona fide monocyte subset [14], as transcriptional profiling has indicated their closer relationship with the monocyte compartment than with the DC compartment [15]. As such, inclusion of SLAN in this panel offers users the ability to examine this subset, distinct from other nonclassical monocytes. A full list of the antibodies used in this panel is given in Table 2.

Figure 1 demonstrates the gating strategy for excluding non-monocytes (Figure 1A) and delineating the four monocyte subsets (Figure 1B). Six markers across three detectors were designated to exclude nonmonocytes. Nonleukocytes (contaminating platelets and red blood cells) were excluded by gating on $CD45^+$ cells (Figure 1A, vii) and granulocytes (neutrophils and eosinophils) were excluded by gating on $CD45^+/CD66b^-$ cells (Figure 1A, viii). Lineage markers for T cells (CD3), B cells (CD19), Natural Killer cells (CD56), and both plasmacytoid DCs and basophils (CD123) were assigned to the same fluorophore (FITC). As such, monocytes were defined as lineage⁻ (Lin^-). In conjunction with these lineage markers, TLR2 was used as a pan-monocyte marker to pull out a clean monocyte population ($TLR2^+/$

TABLE 1 Summary table for application of OMIP-083

Purpose	Delineation of peripheral monocyte subsets and deep phenotyping of monocyte function.
Species	Humans
Cell type	PBMCs
Cross references	OMIP-023, OMIP-024, OMIP-034, OMIP-038, OMIP-042, OMIP-069

TABLE 2 Reagents for OMIP-083

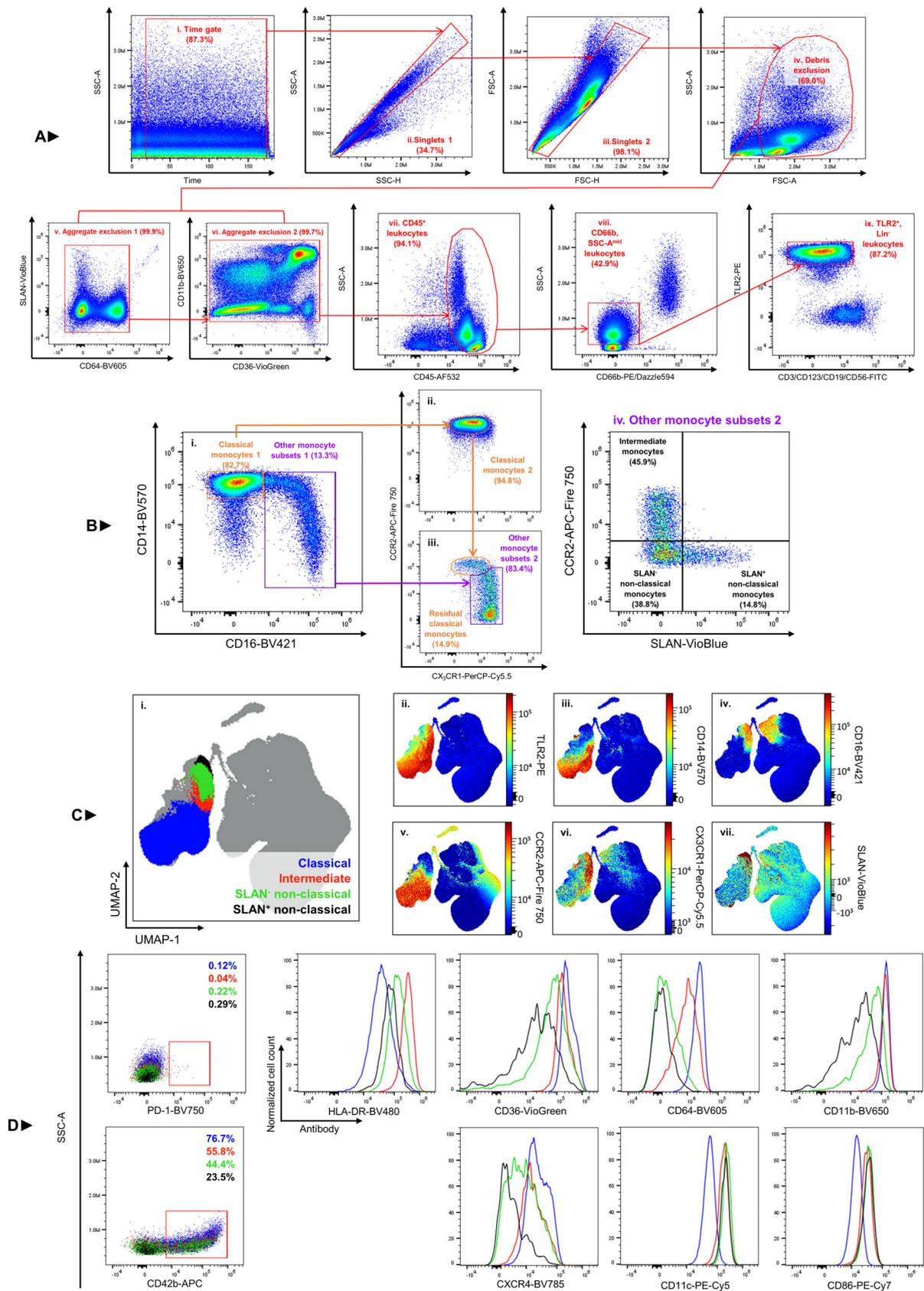| Specificity	Fluorochrome	Clone	Purpose
CD45	Alexa Fluor 532	HI30	ID leukocytes
CD66b	PE-Dazzle 594	G10F5	Exclude neutrophils and eosinophils
CD3	FITC	SK7	Exclude pan-T cells
CD123	FITC	6H6	Exclude basophils and pDCs
CD19	FITC	SJ25C1	Exclude B cells
CD56	FITC	HCD56	Exclude NK cells
TLR2	PE	11G7	ID monocytes, pattern recognition receptor expression
CD14	BV570	M5E2	ID monocyte subsets
CD16	BV421	3G8	ID monocyte subsets, Fc receptor expression
SLAN	VioBlue	DD-1	ID monocyte subsets
CCR2	APC-Fire 750	K036C2	ID monocyte subsets, cytokine receptor expression
CX3CR1	PerCP-Cy5.5	2A9-1	Cytokine receptor expression
CXCR4	BV785	125G	
CD36	VioGreen	AC106	Scavenger receptor expression
CD11c	PE-Cy5	3.9	Adhesion receptor expression
CD11b	BV650	ICRF44	
HLA-DR	BV480	G46-6	Antigen presentation
CD86	PE-Cy7	BU63	
CD42b	APC	HIP1	Heterotypic aggregation
CD64	BV605	10.1	Fc receptor expression
PD-1	BV750	EH12.2H7	Examine the PD-1 pathway

FIGURE 1   Legend on next page.

Lin⁻) (Figure 1A, ix). TLR2 is similarly and highly expressed across classical, intermediate and nonclassical monocytes, noted both here and by others [16–18]. Similar and high expression across subsets is desirable for a pan marker and, here, eliminates HLA-DR (variably expressed) and CD86 (dimly expressed) (**Figure S9** of **Data S1**), both of which are commonly cited as pan-monocyte markers elsewhere [9, 19, 20]. In this panel, the total monocyte population is thus defined as $CD45^+/CD66b^-/Lin^-/TLR2^+$. At this stage of gating (Figure 1A ix), we also eliminate $Lin^-/TLR2^{low}$ cells. As such, we define monocytes as strictly $TLR2^+$.

Having defined total monocytes, close attention must be paid to manually gate each monocyte subset, particularly given that each has distinctive functions. This is commonly achieved by visualizing the total monocyte population by CD14 and CD16 expression (Figure 1B i). The majority of the population is $CD14^{++}/CD16^-$ (an expression pattern that defines classical monocytes) and the remaining "tail" of monocytes (inclusive of both intermediate and nonclassical monocytes) show increasing expression of CD16 and decreasing expression of CD14. The task of manually gating all monocyte subsets by CD14 and CD16 is, thus, difficult as these subsets sit along a gradient of CD14 and CD16 expression. This is a particular problem for defining intermediate monocytes which, by virtue of their name, express an intermediate phenotype between the classical and nonclassical subsets. As such, intermediate monocytes are frequently manually gated from other subsets at an arbitrary level of CD14 and CD16 expression. Our gating strategy accounts for this gradient effect by defining each of the monocyte subsets with a larger set of markers (CD14, CD16, CCR2, CX₃CR1, SLAN) rather than relying solely on CD14 and CD16 expression.

Separating classical monocytes from all other monocytes is routinely and accurately achieved by examining CD16 and CD14 expression (Figure 1B i). As such, classical monocytes are identified as $CD45^+/CD66b^-/Lin^-/TLR2^+/CD14^{++}/CD16^-$. All other subsets are defined in this plot as $CD14^{var}/CD16^{var}$. We also place a confirmatory gate around this classical monocyte population using both CCR2 and CX₃CR1 (Figure 1B, ii): compared to all other monocyte subsets, classical monocytes are $CCR2^{high}/CX_3CR1^{low}$. We additionally apply this confirmatory gate to $CD14^{var}/CD16^{var}$ monocytes to identify and exclude residual classical monocytes (Figure 1B, iii). Also within Figure 1B, iii, the remaining monocyte subsets (intermediate and nonclassical) are gated as $CCR2^{low}/CX_3CR1^{high}$ compared to classical monocytes.

The next task is accurate separation of intermediate and nonclassical monocyte subsets, which requires markers that are differentially expressed between these populations. Markers that satisfy this requirement include CCR2, CXCR4, CD36, and SLAN. Of particular interest, nonclassical monocytes are well-cited as negative for CCR2 [10–12, 21–23], CXCR4 [21, 23] and CD36 [21, 22, 24], whereas intermediate monocytes show variable expression of all three markers. The nonclassical phenotype can therefore be described as $CCR2^-/CXCR4^-/CD36^-$, and are phenotypically distinct from all other monocyte subsets, which can be described as $CCR2^{var}/CXCR4^{var}/CD36^{var}$. As described earlier, the addition of SLAN also allows for discrimination of two nonclassical populations ($SLAN^+$ vs. $SLAN^-$). In our hands, CCR2 worked best for identifying nonclassical ($CCR2^-$) away from intermediate ($CCR2^+$) monocytes, compared to both CXCR4 and CD36 (**Figure S11** of **Data S1**) and were therefore defined as shown in Figure 1B, iv. Intermediate monocytes are thus identified as $CD45^+/CD66b^-/Lin^-/TLR2^+/CD14^+/CD16^+/CX_3CR1^{low}/CCR2^+$. In conjunction with SLAN, $CCR2^-$ nonclassical monocytes could be further delineated into $SLAN^+$ ($CD45^+/CD66b^-/Lin^-/TLR2^+/CD14^-/CD16^{++}/CX_3CR1^{low}/CCR2^-/SLAN^+$) and $SLAN^-$ ($CD45^+/CD66b^-/Lin^-/TLR2^+/CD14^-/CD16^{++}/CX_3CR1^{low}/CCR2^-/SLAN^-$) subsets. Based on **Figure 1A,B**, all four monocyte subsets can be defined using 12 markers (CD45, CD66b, CD3, CD19, CD56, CD123, TLR2, CD14, CD16, CCR2, CX₃CR1, SLAN) across nine detectors. In Figure 1B, i, there is a population of $CD14^{low}CD16^-$; these cells are excluded from analysis as their expression pattern of both CD14 and CD16 is uncharacteristic of monocytes.

$CD45^+$ events from each of six PBMC samples were combined to visualize the four manually gated monocyte subsets using the UMAP algorithm (Figure 1C, i) [25]. Heatmap overlays for TLR2, CD14,

FIGURE 1 Overview of the 21-marker, 18-color monocyte-centric panel on human PBMCs. PBMCs were density-separated from Cyto-Chex blood collection tubes (Streck, La Vista, NE), stained and acquired on a 3-laser Cytek Aurora (Cytek biosciences, Fremont, CA). Initially, the sample is cleaned by excluding variable flow rate during acquisition (typically experienced at the start and end of sample acquisition), doublets, debris and antibody aggregates (A, i-vi). Following cleaning, $CD45^+$ (A, vii) and $CD66b^-$ (A, viii) leukocytes are sequentially gated. Several lineage markers (CD3, CD19, CD56, CD123) are conjugated to the same fluorochrome to facilitate efficient exclusion of all other nonmonocyte cells (A, ix). Within the same plot that Lin^+ leukocytes are excluded, the monocyte population is defined as $TLR2^+$ (A, ix). As such, the monocyte population is defined as: $CD45^+/CD66b^-/Lin^-/TLR2^+$. Monocytes display their characteristic expression of CD14 and CD16 (B, i). Separating classical ($CD14^{++}/CD16^-$) monocytes from all other monocyte subsets ($CD14^{var}/CD16^{var}$) can be achieved in this plot. From here, classical monocytes are confirmed to display their expected pattern of CCR2 and CX₃CR1 (B, ii). Residual classical monocytes are defined in B, iii as those cells which were originally gated as 'other monocyte subsets' from the parent population but which subsequently show CCR2 and CX₃CR1 expression patterns identical to classical monocytes. This population is removed from downstream analysis. From here, a true population of 'other monocyte subsets' is defined (B, iii) and subsequently divided into intermediate ($CCR2^+/SLAN^-$) monocytes and two subsets of nonclassical monocytes based on expression of SLAN: $SLAN^+$ ($CCR2^-/SLAN^+$) nonclassical and $SLAN^-$ ($CCR2^-/SLAN^-$) monocytes (B, iv). High-dimensional analysis with the UMAP algorithm was conducted on PBMCs from two individuals across three timepoints (for a total of six samples) (C). Data were cleaned (as demonstrated in A, i-vi) and $CD45^+$ events from these six samples were combined and used for this analysis. Manual gating of the four monocyte populations was overlaid on this two-dimensional rendering (C, i). UMAP analysis demonstrates the ease of discriminating the monocyte population from all other leukocytes using TLR2 (C, ii). Heatmap overlays also demonstrate the distinct expression levels of CD14 (C, iii), CD16 (C, iv), CCR2 (C, v), CX₃CR1 (C, vi) and SLAN (C, vii) within these monocyte populations. Once identified, these four monocyte subsets were interrogated for their expression of a further nine markers (D); each monocyte subset shows distinctive expression profiles

CD16, CCR2, CX$_3$CR1, and SLAN (Figure 1C, ii-vii) demonstrate the differential expression patterns across the four monocyte subsets. In Figure 1C, i and ii, we can see that TLR2^{low} cells are excluded from analysis; strictly TLR2$^+$ cells are defined as monocytes.

Having identified these four subsets, we can interrogate various effector functions including: 1) heterotypic aggregation (CD42b), 2) adhesion (CD11b, CD11c), 3) pattern recognition (TLR2), 4) antigen presentation (HLA-DR, CD86), 5) the PD-1 pathway (PD-1), 6) chemokine receptor expression (CCR2, CX$_3$CR1, CXCR4), 7) Fc receptor expression (CD16, CD64) and 8) scavenging receptor expression (CD36). The expression patterns of these markers across each monocyte subset are shown in Figure 1D. This is a nonexhaustive list but provides a broad overview of monocyte function. If users were interested in probing other functions, we suggest using the 12 core markers for defining each subset and, from here, any markers of interest could be swapped in or, in the case of additional lasers, added alongside the functional markers listed above.

Optimization was conducted on peripheral blood anticoagulated and preserved in Cyto-Chex BCTs (Streck). Preserving at the time of blood draw allows for a 'snapshot' of cellular phenotyping that is not provided by other BCTs, where storage time before processing may influence live cell phenotyping. The use of a preservative eliminates the use of a viability dye in this panel (Figure S3 of Data S1) but, if other BCTs were used, we suggest that Zombie-NIR (BioLegend, San Diego, CA) could be added to this panel without further optimization. As our ultimate goal is to use this panel for assessing monocyte immune status as it relates to disease course in our model of interest, we prioritized the use of this BCT over more traditional anticoagulants (e.g., ethylenediaminetetraacetic acid [EDTA]). This allows for potentially extended times between blood draw and processing, which is the type of flexibility required for clinical blood processing. However, cells collected in these tubes, being preserved, are not appropriate for downstream functional assays. We believe this panel could be used on blood anticoagulated with EDTA or another anticoagulant of choice with minimal optimization, which would provide the opportunity to interrogate monocytes *in vitro* if required by the user.

Troubleshooting of this panel centered on four aspects: 1) optimizing a core panel that is crucial for enumerating each monocyte subset, 2) choice of reagents used during isolation and staining of cells, 3) investigating sequential staining for selected markers, and 4) investigating alternative fluorochrome choices where necessary. To clearly present this information to the reader, we have constructed two supplementary materials. **Data S1** focuses on panel optimization and marker-fluorochrome selection. **Data S2** focuses on the steps taken to optimize the staining pattern of a subset of monocyte-centric markers included in this 21-marker, 18-color panel. During troubleshooting, particular attention was paid to optimizing staining of CD16, a crucial monocyte marker, which was ultimately resolved by systematically reviewing alternative fluorochromes, staining reagents and the protocol for isolating cells from peripheral blood (Figures S1–S4 of **Data S2**). Second to this, alternative staining protocols were trialed for the three cytokine receptors (CCR2, CX$_3$CR1, CXCR4) as well as CD14 and, ultimately, these four markers were sequentially stained to achieve optimal results (**Figures S5** and **S6**

of **Data S2**). We also outline our decision regarding which single-stained controls (cell versus beads) should be used for unmixing this monocyte-centric panel (**Figures S14–S16** of **Data S1**). The final staining protocol is outlined in **Section S15** of **Data S1**.

In summary, our 21-marker, 18-color monocyte-centric panel is designed to identify four peripheral monocyte subsets and interrogate monocyte phenotype across a wide range of functional pathways. This panel consists of a core of 12 markers across nine fluorochromes (CD45, CD66b, CD3, CD19, CD56, CD123, TLR2, CD14, CD16, CCR2, CX$_3$CR1, and SLAN) to delineate these subsets and a further nine markers (CXCR4, CD36, CD11c, CD11b, HLA-DR, CD86, CD42b, CD64, PD-1) can be used to probe monocyte immune status across eight unique functional pathways (Table 2). This panel has broad applicability to study inflammatory conditions that are known to induce changes in monocyte phenotype and can be used to determine the clinical utility of deep monocyte phenotyping for predicting disease course.

1.1 | Similarity to published OMIPs

Several published OMIPs (OMIP-023 [3], OMIP-024 [4], OMIP-034 [5], OMIP-038 [6], OMIP-042 [7], OMIP-069 [1]), which broadly aim to characterize major leukocyte subsets in human peripheral blood, gate on the monocyte population. Most gate on the monocyte population using one or a combination of CD14 and HLA-DR (OMIP-023 [3], OMIP-024 [4], OMIP-034 [5], OMIP-038 [6], OMIP-042 [7]). Similarly, most also identify the three monocyte populations (classical, intermediate, nonclassical) using both CD14 and CD16 (OMIP-023 [3], OMIP-024 [4], OMIP-038 [6], OMIP-069 [1]). Here, we expand on these definitions for each monocyte subset, provide an alternative gating strategy for identifying these subsets and demonstrate how this panel can be utilized to analyze monocyte phenotype in-depth.

1.2 | Human subjects

Whole blood was obtained from healthy volunteers under ethical approval (19/CEN/129) by the Health and Disability Ethics Committee, New Zealand.

AUTHOR CONTRIBUTIONS

Kathryn E. Hally: Conceptualization (lead); data curation (lead); formal analysis (equal); writing – original draft (lead); writing – review and editing (equal). **Laura Ferrer-Font:** Conceptualization (supporting); data curation (supporting);

formal analysis (equal); writing – original draft (supporting); writing – review and editing (equal). **Katherine R. Pilkington:** Conceptualization (supporting); data curation (supporting); formal analysis (equal); writing – original draft (supporting); writing – review and editing (equal). **Peter D. Larsen:** Conceptualization (supporting); data curation (supporting); formal analysis (equal); writing – original draft (supporting); writing – review and editing (equal).

CONFLICT OF INTEREST

Katherine Pilkington is an employee of Cytek Biosciences, Inc., the manufacturer of the Aurora full spectrum flow cytometer used in this manuscript.

PEER REVIEW

The peer review history for this article is available at https://publons.com/publon/10.1002/cyto.a.24545.

ORCID

Kathryn E. Hally https://orcid.org/0000-0003-3608-3795
Laura Ferrer-Font https://orcid.org/0000-0002-3131-7233
Katherine R. Pilkington https://orcid.org/0000-0002-1848-1645
Peter D. Larsen https://orcid.org/0000-0001-8706-9032

REFERENCES

1. Park LM, Lannigan J, Jaimes MC. OMIP-069: forty-color full Spectrum flow cytometry panel for deep Immunophenotyping of major cell subsets in human peripheral blood. Cytometry A. 2020;97(10):1044–51.
2. Niewold P, Ashhurst TM, Smith AL, King NJC. Evaluating spectral cytometry for immune profiling in viral disease. Cytometry A. 2020;97(11):1165–79.
3. Bocsi J, Melzer S, Dähnert I, Tárnok A. OMIP-023: 10-color, 13 antibody panel for in-depth phenotyping of human peripheral blood leukocytes. Cytometry A. 2014;85(9):781–4.
4. Moncunill G, Han H, Dobaño C, McElrath MJ, De Rosa SC. OMIP-024: pan-leukocyte immunophenotypic characterization of PBMC subsets in human samples. Cytometry A. 2014;85(12):995–8.
5. Baumgart S, Peddinghaus A, Schulte-Wrede U, Mei HE, Grätzkau A. OMIP-034: comprehensive immune phenotyping of human peripheral leukocytes by mass cytometry for monitoring immunomodulatory therapies. Cytometry A. 2017;91(1):34–8.
6. Smolen KK, Cai B, Kollmann TR. OMIP-038: innate immune assessment with a 14 color flow cytometry panel. Cytometry A. 2017;91(10):966–8.
7. Staser KW, Eades W, Choi J, Karpova D, DiPersio JF. OMIP-042: 21-color flow cytometry to comprehensively immunophenotype major lymphocyte and myeloid subsets in human peripheral blood. Cytometry A. 2018;93(2):186–9.
8. Ziegler-Heitbrock L, Ancuta P, Crowe S, Dalod M, Grau V, Hart DN, et al. Nomenclature of monocytes and dendritic cells in blood. Blood. 2010;116(16):e74–80.
9. Weber C, Shantsila E, Hristov M, Caligiuri G, Guzik T, Heine GH, et al. Role and analysis of monocyte subsets in cardiovascular disease. Joint consensus document of the European Society of Cardiology (ESC) Working Groups "Atherosclerosis & Vascular Biology" and "Thrombosis". Thromb Haemost. 2016;116(4):626–37.
10. Cros J, Cagnard N, Woollard K, Patey N, Zhang SY, Senechel B, et al. Human CD14dim monocytes patrol and sense nucleic acids and viruses via TLR7 and TLR8 receptors. Immunity. 2010;33(3):375–86.
11. Roussel M, Ferrell PB Jr, Greenplate AR, Lhomme F, Le Gallou S, Diggins KE, et al. Mass cytometry deep phenotyping of human mononuclear phagocytes and myeloid-derived suppressor cells from human blood and bone marrow. J Leukoc Biol. 2017;102(2):437–47.
12. Wong KL, Tai JJ, Wong WC, Han H, Sem X, Yeap WH, et al. Gene expression profiling reveals the defining features of the classical, intermediate, and nonclassical human monocyte subsets. Blood. 2011;118(5):e16–31.
13. Hamers AAJ, Dinh HQ, Thomas GD, Marcovecchio P, Blatchley A, Nakao CS, et al. Human monocyte heterogeneity as revealed by high-dimensional mass cytometry. Arterioscler Thromb Vasc Biol. 2019;39(1):25–36.
14. Ahmad F, Döbel T, Schmitz M, Schäkel K. Current concepts on 6-sulfo LacNAc expressing monocytes (slanMo). Front Immunol. 2019;10(948).
15. van Leeuwen-Kerkhoff N, Lundberg K, Westers TM, Kordasti S, Bontkes HJ, de Gruijl TD, et al. Transcriptional profiling reveals functional dichotomy between human slan+ non-classical monocytes and myeloid dendritic cells. J Leukoc Biol. 2017;102(4):1055–68.
16. Shirk EN, Kral BG, Gama L. Toll-like receptor 2(bright) cells identify circulating monocytes in human and non-human primates. Cytometry A. 2017;91(4):364–71.
17. Sabroe I, Jones EC, Usher LR, Whyte MKB, Dower SK. Toll-like receptor (TLR)2 and TLR4 in human peripheral blood granulocytes: a critical role for monocytes in leukocyte lipopolysaccharide responses. J Immunol. 2002;168(9):4701.
18. Kurt-Jones EA, Mandell L, Whitney C, Padgett A, Gosselin K, Newburger PE, et al. Role of toll-like receptor 2 (TLR2) in neutrophil activation: GM-CSF enhances TLR2 expression and TLR2-mediated interleukin 8 responses in neutrophils. Blood. 2002;100(5):1860–8.
19. Heimbeck I, Hofer TPJ, Eder C, Wright AK, Frankenberger M, Marei A, et al. Standardized single-platform assay for human monocyte subpopulations: lower CD14+CD16++ monocytes in females. Cytometry A. 2010;77A(9):823–30.
20. Zawada AM, Rogacev KS, Schirmer SH, Sester M, Böhm M, Fliser D, et al. Monocyte heterogeneity in human cardiovascular disease. Immunobiology. 2012;217(12):1273–84.
21. Mueller KAL, Hanna DB, Ehinger E, Xu X, Baas L, Gawaz MP, et al. Loss of CXCR4 on non-classical monocytes in participants of the Women's interagency HIV study (WIHS) with subclinical atherosclerosis. Cardiovasc Res. 2019;115(6):1029–40.
22. Tallone T, Turconi G, Soldati G, Pedrazzini G, Moccetti T, Vassalli G. Heterogeneity of human monocytes: an optimized four-color flow cytometry protocol for analysis of monocyte subsets. J Cardiovasc Transl Res. 2011;4(2):211–9.
23. Shantsila E, Wrigley B, Tapp L, Apostolakis S, Montoro-Garcia S, Drayson MT, et al. Immunophenotypic characterization of human monocyte subsets: possible implications for cardiovascular disease pathophysiology. J Thromb Haemost. 2011;9(5):1056–66.
24. Mukherjee R, Kanti Barman P, Kumar Thatoi P, Tripathy R, Kumar Das B, Ravindran B. Non-classical monocytes display inflammatory features: validation in sepsis and systemic lupus erythematous. Sci Rep. 2015;5(1):13886.
25. McInnes L, Healy J, Saul N, Großberger, L. UMAP: uniform manifold approximation and projection. J Open Source Softw. 2018;3(29):861.

SUPPORTING INFORMATION

Additional supporting information may be found in the online version of the article at the publisher's website.